Interferometry

PHYS4796 Lab Writeup

Maya Desai and Jose Mendez

ABSTRACT

The Michelson and Sagnac interferometers are devices that utilize the phenomena of light interference to make sensitive measurements. Here, a Michelson interferometer was assembled to measure the magnetostriction of a nickel rod. The sample constricted as the magnetic field strength H was increased and a saturation curve was obtained, although our device could not reach the magnetostriction coefficient of nickel of $\lambda_s = -(5.0 \; - \; 5.2) \times 10^{-6}$ (m/m)(A/mm). A Sagnac interferometer was assembled to observe the Pockels electro-optic effect in a $LiNbO_3$ crystal. A difference in the index of refraction as a result of an applied electric field was observed. Our experiments demonstrate the usefulness of interferometry to measure material properties. (118)

INTRODUCTION

The Michelson interferometer was invented by American physicist Albert A. Michelson around 1880. He and physicist Edward W. Morley wanted to measure Earth's velocity relative to the "luminiferous aether," a medium they though may exist throughout space and carry light waves. [1] They pointed a laser through a beamsplitter to obtain two mutually phased coherent beams. The resulting reflected and transmitted beams were then sent back by two mirrors and recombined. If the light was traveling through ether, light traveling in perpendicular directions would have different speeds, and their waves would interfere when recombined. The Michelson-Morley was unsuccessful in showing the existence of ether, however their device remains useful. For example, since the appearance of the interference fringes is sensitive to the inequality of the distances to each mirror, the Michelson interferometer is used to measure lengths precisely. Additionally, the Laser Interferometer Gravitational-wave Observatory (LIGO) used a Michelson interferometer for their measurement of gravitational waves.

In 1913, French Physicist Georges Sagnac expanded on Michelson and Morley's attempt to show the existence of ether by constructing an interferometer with a single inertial reference frame, which was what he believed lacked in Michelson's device. [2] In Sagnac's interferoemeter, the two split beams emerge are directed around a ring of multiple mirrors in opposite directions and then recombined. Sagnac's experiment did not show the existence of ether either, but also still has many applications. For example, since the Sagnac is sensitive to rotations, it can be used to take the rotation of the earth into account for technology such as global navigation satellite systems and clock synchronization. [2]

BACKGROUND

Interference

These two interferometers rely on the property of light interference. When two beams of light overlap, their waves interfere. If they interfere with a slight difference in phase, an interference pattern can be observed in their projection.

In a Sagnac interferometer and unequal-arm Michelson interferometer, the two recombined beams of light have traveled different distances. This causes a parallel straight fringe pattern. In an equal-arm Michelson interferometer, the two beams of light travel equal distances but their spherical wavefronts have different radii of curvature. This causes a bullseye interference pattern.

These two interference patterns are displayed in Fig. 1. [3]

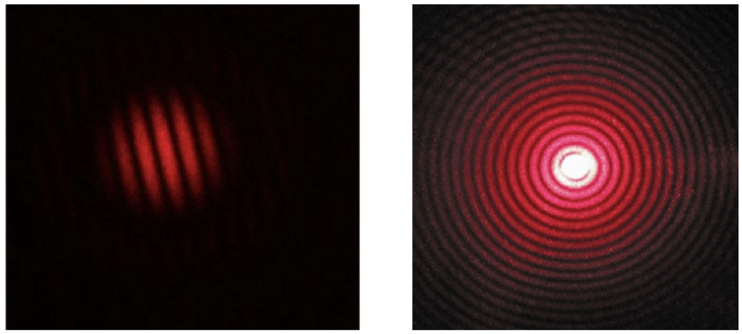

(a) (b)

Figure 1: Fringe (a) and bullseye (b) interference patterns of red light occur from the Sagnac and Michelson interferometer, respectively. Image taken from [3]

Magnetostriction

Magnetostriction is the property of ferromagnetic substances to change shape as a result of an applied magnetic field. This occurs because ferromagnetic materials consist of regions with uniform magnetization, or unidirectional magnetic dipoles. When an external magnetic field is applied, the magnetization of these regions changes, causing its lattice to distort. This distortion is represented by the magnetostrictive coefficient λ, measured in units of microstrains. One microstrain is defined by Eq (1),

$$\lambda = \frac{\Delta L}{L} \times 10^{-6} \tag{1}$$

where L and ΔL are the original length and change in length respectively. The magnetostrictive coefficient can be positive or negative, corresponding to an expansion or constriction under an applied magnetic field respectively. As the magnetic field is increased, the effect reaches saturation, represented by the saturation magnetostrictive constant λ_s.

The dimensional changes due to magnetostriction are not large. Since the Michelson interferometer, depicted in Fig. 3 and described under *Methods*, is sensitive to the path length difference of its arms, it is a well-suited measurement device of magnetostriction. The laser output signal S from a Michelson interferometer as a function of the change in length ΔL of one of its arms is given by Eq (2),

$$S(f, \Delta L) = S(f, 0)\cos^2(\frac{2\pi f}{c}\Delta L) \tag{2}$$

where f is the input beam frequency, $S(f, 0)$ is the equal-arm signal, and c is the speed of light. The oscillating intensity is a result of interference fringes appearing or disappearing. Thus in order to calculate ΔL we can use Eq (3),

$$\Delta L = n\frac{\lambda}{2} \tag{3}$$

where n is the number of added or subtracted interference fringes and λ is the wavelength of light.

To supply the magnetic field to our material, we surrounded a sample rod with a solenoid and applied a current. The magnetic intensity field H of a solenoid with turn density n and current I as a function of time t is given by Eq (4).

$$H(t) = n\ I(t) \tag{4}$$

A comparison of the magnetic field H against relative length change $\Delta L/L$ results in a characteristic saturation curve depending on the material. Fig. 2 displays some example magnetostriction curves for various ferromagnetic materials. [4]

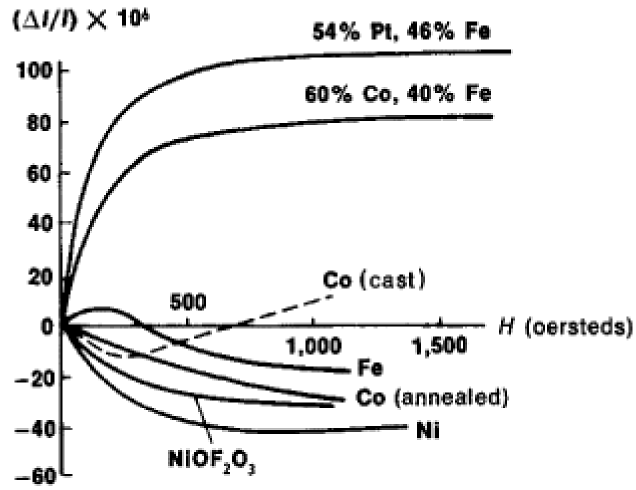

Figure 2: Magnetostriction curves for various ferromagnetic materials. Figure taken from [4]

The Pockels Electro-optic Effect

Electro-optic effects refer to the changes in the optical properties of some materials in response to an applied electric field. In the Pockels electro-optic effect, an applied electric field causes the refractive index of a crystal to change. This occurs in crystals that lack inversion symmetry, the property of a lattice to be identical to its mirror image.

We used the Sagnac interferometer to measure this effect, depicted in Fig. 7 and described under *Methods*. The phase shift of the laser beams $\Delta\phi$ relates to the change in refractive index Δn by Eq (5),

$$\Delta\phi = \frac{2\pi\Delta n}{\lambda_{vac}} L \tag{5}$$

where L is the length of the crystal and λ_{vac} is the laser wavelength in a vacuum.

METHODS

Measuring Magnetostriction with the Michelson Interferometer

We assembled a Michelson interferometer by splitting a beam with a dielectric cube beamsplitter, reflecting the two beams back through the beamsplitter with two mirrors, and measuring their interference condition with a photodetector. The schematic is depicted in Fig. 3.

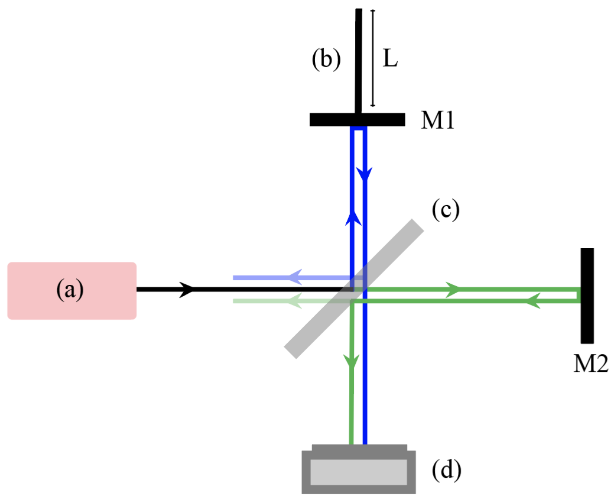

Figure 3: Schematic of the Michelson interferometer
(a) HeNe Light source
(b) Adjustable length micrometer with external controller
(c) Dielectric beamsplitter: splits a beam of light into a transmitted and a reflected beam
(d) Photodetector
(M1), (M2) Mirrors

.

The path length was adjusted by adjusting the length of the micrometer (L) until a bullseye interference pattern was observed at location (d). This ensured that the two arms of the interferometer were equal in length.

Then, a second beamsplitter was inserted as shown in Fig. 4. This configuration is called the quadrature Michelson interferometer and allows for measurements of path length changes.

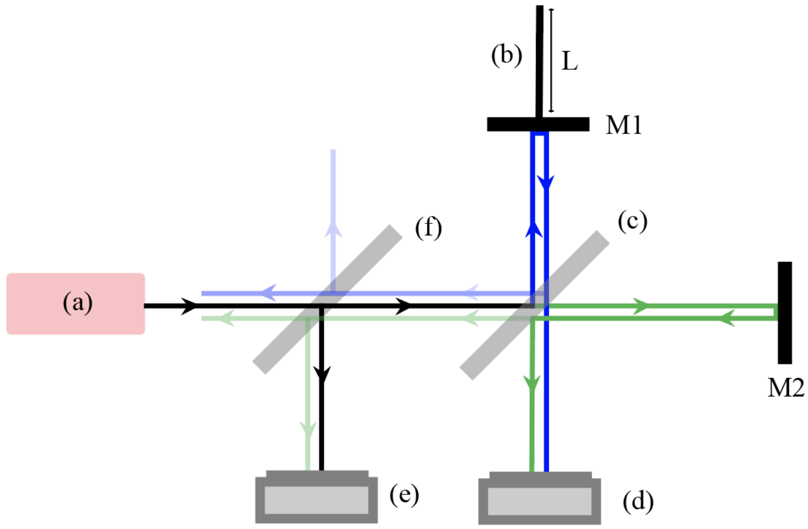

Figure 4: Quadrature Michelson interferometer
(e) Second photodetector
(f) Second dielectric polarizer
(M1), (M2) Mirrors

.

The external controller for the micrometer was turned on to slowly increase the path length. Using an oscilloscope connected to the photodetectors (d) and (e), we observed the changing phases of the waves. In XY mode, we could observe the elliptical locus this phase shift creates, depicted by Fig. 5.

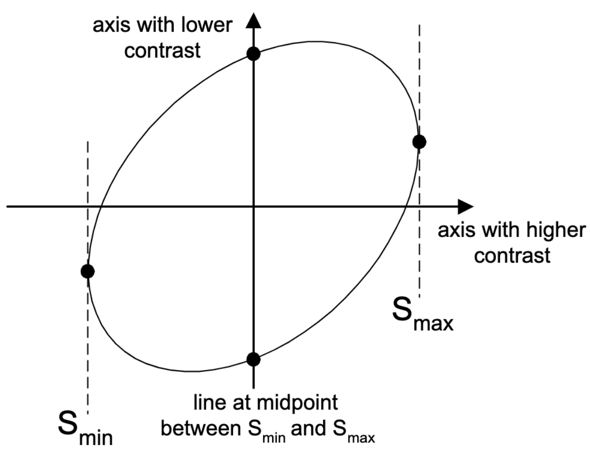

Figure 5: Eliptical locus observed by slowly changing one arm length of the Michelson interferometer

The micrometer was then replaced with a 295 mm Alloy-200 nickel rod surrounded by a copper solenoid, and mirror M1 was replaced by a mirror on a flexure stage, shown in Fig. 6.

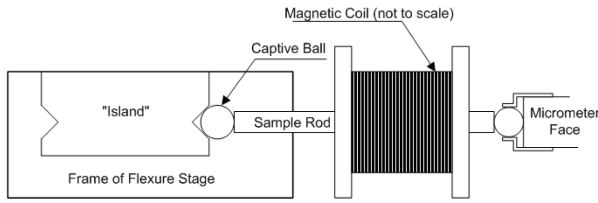

Figure 6: Device to measure magnetostriction. A nickel rod surrounded by a magnetic coil and attached to a mirror on a flexure stage is placed at location (b) in Fig. 4.

The solenoid had 2400 ± 60 turns, and the controller could provide current up to 3 A. By Eq (4), H could reach a maximum of 43.8×10^3 A/m. The current was slowly increased to its maximum and then decreased back to its minimum. The currents at which the minimum signals from photodetector (e) were recorded. From one minimum to the next represented one new interference fringe, n.

We could then plot H as a function of $\Delta L/L$ to obtain a magnetostriction curve.

Measuring the Pockels Electro-optic Effect with the Sagnac Interferometer

To observe the Pockels effect, we assembled a Sagnac Interferometer, as depicted in the schematic Fig. 7. First, the interferometer was aligned so that the beams overlapped at all points. Then, the vertical position of M2 was adjusted using the stage (e) so that the beams separated within the loop but still overlapped when entering the detector. Then, an $8 \times 8 \times 15$ mm sample of $LiNbO_3$ was placed in the path of one of the beams. Capacitor plates were attached to either side of the crystal and set to provide a square wave of voltage.

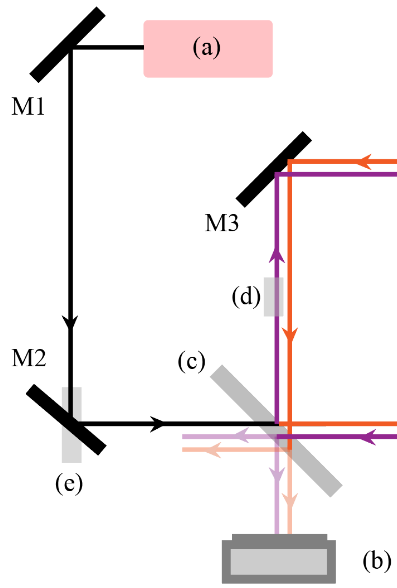

Figure 7: Sagnac Interferometer
(a) 632.8 nm HeNe laser source
(b) Photodetector
(c) Polarizing beamsplitter cube
(d) $LiNbO_3$ sample surrounded by capacitor plates
(e) Rack and pinion adjustable stage
(M1-5) Mirrors

.

We inserted an additional angled beamsplitter and angled mirror into the setup in Fig. 7 to split the horizontal and vertical components of the beam into two photodetectors. Then, by attaching an oscilloscope to the photodetectors we could observe the changes in signal from the interferometer.

RESULTS AND ANALYSIS

Measuring Magnetostriction with the Michelson Interferometer

The current values at which each minimum signal occurred, as well as their corresponding H values calculated using Eq (4), are listed in Table 1. We found that as the current was increased, the number n of visible diffraction fringes decreased, meaning nickel constricts as a DC magnetic field is increased and vice versa.

		Increasing A		Decreasing A	
	ΔL(nm)	$I_{min}(A)$	H (A/mm)	$I_{min}(A)$	H (A/mm)
Trial 1	-317	0.23	1.9	0.25	2.1
	-633	0.76	6.2	0.75	6.2
	-950	1.5	12	1.75	14
Trial 2	-317	0.30	2.5	0.25	2.1
	-633	1.0	8.2	0.75	6.2
	-950	1.5	12	2.0	16

Table 1: Change in length at different magnetic field strengths and in different directions

The data in Table 1 are plotted in Fig. 8. As expected, we can extrapolate a negative curve that should reach saturation as the DC magnetic field is increased. Our apparatus did not allow a high enough magnetic field to observe the complete saturation at an accepted value of $\lambda_s = -(5.0 - 5.2) \times 10^{-6}$ (m/m)(A/mm).

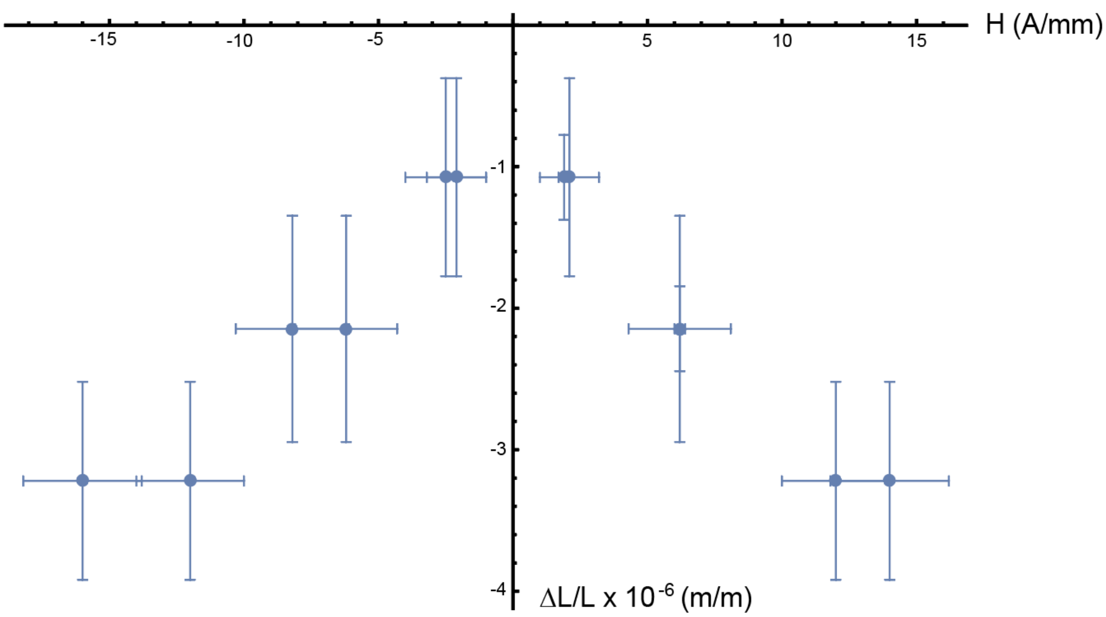

Figure 8: Magnetostriction of nickel as a function of applied magnetic field H

.

The leading sources of error in these measurements come from human estimation of the fringe changes and minimums, and phase instability in the interferometer.

Measuring the Pockels Electro-optic Effect with the Sagnac Interferometer

We applied a square wave to the applied voltage and observed a square wave change in signal in our oscilloscope, demonstrating that the Pockel's electro-optic effect occurred.

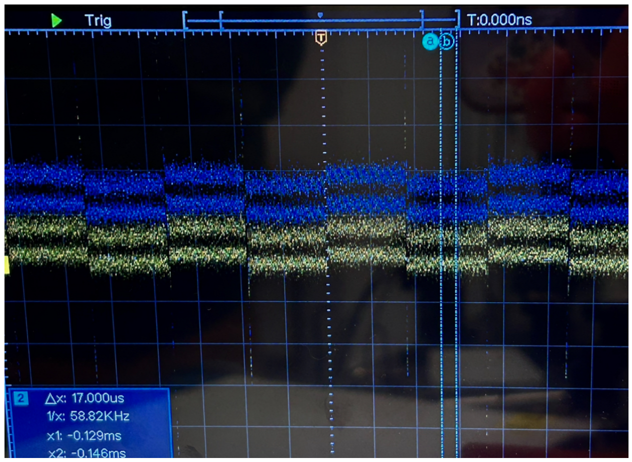

Figure 9: Square waves observed on the oscilloscope as a result of oscillating the applied electric field on the crystal

.

Despite the theoretical property of stability of the Sagnac interferometer, we were unable to obtain a stable signal. Our system was incredibly sensitive to external vibrations and air currents. This noise prevented us from making quantitative measurements. Future measurements could be taken in a more controlled environment to attempt the precise measurements the Sagnac interferometer can theoretically achieve.

CONCLUSION

We assembled a Michelson interferometer the measure magnetostriction of a nickel rod. We observed that the length of the Nickel rod constricted as the magnetic field strength was increased and obtained a saturation curve that could reasonably trend towards the saturation coefficient of $-(5.0\,-\,5.2)\times10^{-6}$ (m/m)(A/mm). Precise knowledge of the magnetostriction behavior of metals has many engineering applications, such as magnetic field sensors and transformers.

We used the Sagnac interferometer to observe the Pockel's electro-optic effect for a sample of single-crystal lithium niobate. The Pockel's effect states that the application of an electric field to crystals lacking inversion symmetry induces a change in its index of refraction. Pockels cells have many applications, such as two-photon excitation microscopy, a technique of fluorescence imaging used to image living tissue. We observed that applying a square wave electric field to the sample indeed caused a square wave signal from the interferometer, demonstrating that the Pockel's effect occurred. Our apparatus was unfortunately incredibly sensitive to external noise and vibrations.

Our experiments demonstrate the potential for interferometers to make precise measurements of the properties a variety of materials for various applications. Future work could include the construction of interferometers in more stable spaces with less vibrational noise in order to make more precise measurements.

REFERENCES

[1] D.M. Livingston, Title The Master of Light: A Biography of Albert A. Michelson (Chicago: University of Chicago Press, 1973).

[2] B. Barrett, R. Geiger, et. al. The Sagnac Effect: 20 Years of Development in Matter-wave Interferometry (Comptes Rendus Physique 15, 2014).

[3] Basics of Interferometry (Center for High Angular Resolution Astronomy,)

[4] A. Yu. Romanov and V. P. Silin, The Magnetostriction of Invar alloys (American Institute of Physics 113, 1998)